View metadata, citation and similar papers at core.ac.uk
brought to you by CORE
provided by Elsevier - Publisher Connector

Chinese Journal of Aeronautics, (2014),27(4): 1030–1036

Chinese Society of Aeronautics and Astronautics
& Beihang University

Chinese Journal of Aeronautics

cja@buaa.edu.cn
www.sciencedirect.com

Electrochemical micromachining of micro-dimple arrays on cylindrical inner surfaces using a dry-film photoresist

Qu Ningsong [a,b,*], **Chen Xiaolei** [a], **Li Hansong** [a], **Zeng Yongbin** [b]

[a] *College of Mechanical and Electrical Engineering, Nanjing University of Aeronautics and Astronautics, Nanjing 210016, China*
[b] *Jiangsu Key Laboratory of Precision and Micro-Manufacturing Technology, Nanjing 210016, China*

Received 18 September 2013; revised 2 December 2013; accepted 20 December 2013
Available online 18 March 2014

KEYWORDS

Dry-film photoresist;
Electrochemical machining;
Electrochemical micromachining;
Inner surface;
Micro-dimple arrays;
Texture

Abstract The application of surface textures has been employed to improve the tribological performance of various mechanical components. Various techniques have been used for the application of surface textures such as micro-dimple arrays, but the fabrication of such arrays on cylindrical inner surfaces remains a challenge. In this study, a dry-film photoresist is used as a mask during through-mask electrochemical micromachining to successfully prepare micro-dimple arrays with dimples 94 μm in diameter and 22.7 μm deep on cylindrical inner surfaces, with a machining time of 9 s and an applied voltage of 8 V. The versatility of this method is demonstrated, as are its potential low cost and high efficiency. It is also shown that for a fixed dimple depth, a smaller dimple diameter can be obtained using a combination of lower current density and longer machining time in a passivating sodium nitrate electrolyte.

© 2014 Production and hosting by Elsevier Ltd. on behalf of CSAA & BUAA.
Open access under CC BY-NC-ND license.

1. Introduction

The application of surface textures has been employed to improve the tribological performance of various mechanical components. For example, Kligerman et al. found that partial surface texturing improved the tribological performance of piston rings.[1] Typical surface textures are micro-dimple arrays, prism arrays, pyramid arrays, and micro-grooves, among which micro-dimple arrays have received most attention because the excellent results achieved. Nakano et al. reported that the friction coefficient increases or decreases depending on the geometry of the micro-texture pattern and that lower friction coefficient can be obtained with micro-dimple arrays than with groove- or mesh-patterned textures.[2] Bruzzone et al. found that reductions in friction of 30% or more were feasible with a dimpled surface.[3]A more detailed study by Greco et al., investigating the influence of dimpled surfaces, revealed that the dimensions and layout of the features must be precisely controlled to optimize performance.[4]

* Corresponding author at: College of Mechanical and Electrical Engineering, Nanjing University of Aeronautics and Astronautics, Nanjing 210016, China. Tel.: +86 25 84893870.
E-mail address: nsqu@nuaa.edu.cn (N. Qu).

Peer review under responsibility of Editorial Committee of CJA.

Production and hosting by Elsevier

http://dx.doi.org/10.1016/j.cja.2014.03.012

1000-9361 © 2014 Production and hosting by Elsevier Ltd. on behalf of CSAA & BUAA. Open access under CC BY-NC-ND license.

To generate micro-dimple arrays, several micro-texturing techniques, such as mechanical machining, ion-beam texturing, laser texturing, chemical etching, and electrochemical machining (ECM), can be employed. Compared with other methods, ECM is a promising machining technique, with advantages such as high machining efficiency, independence of material hardness and toughness, the absence of a heat-affected layer, a lack of residual stresses, cracks, tool wear and burrs and low production cost.[5–7] The fabrication of micro-dimple arrays by ECM can involve maskless or through-mask material removal. Natsu et al. prepared micro-dimple arrays 300 μm in diameter by electrolyte jet machining without a mask.[8] Nouraeiz and Roy presented a method of maskless electrochemical microfabrication, in which the anode is placed in an electrochemical reactor close to the cathode carrying the micropattern.[9] Costa and Hutchings fabricated micro-dimple arrays with a feature diameter of 120 μm using a maskless electrochemical texturing method.[10] Byun et al. prepared dimples 300 μm in diameter and 5 μm in depth on a workpiece using the micro-ECM technique, with a tool electrode diameter of 275 μm.[11] This method of machining is simple in comparison with photolithographic processes, but is time-consuming because the dimples are fabricated point by point.

Through-mask electrochemical micromachining (TMEMM) is a commonly used ECM method for the generation of micro-dimple arrays. TMEMM employs photolithography to produce micro-patterns on photoresist-coated substrates, with the process involving a soft bake to dry off the solvent after spin coating, exposure to ultraviolet (UV) light, a post-exposure bake, and photoresist developing. The metal is then selectively dissolved from the unprotected areas.[12] However, the preparation of micro-dimple arrays on non-planar surfaces remains a problem, because it is difficult to use photolithography with such surfaces. Wang and co-workers presented a new method for the fabrication of large-scale micro-dimple arrays on cylindrical objects using proximity rolling-exposure lithography and electrochemical micromachining, in which a cylindrical rod covered with photoresist was sub-area-exposed to a collimated UV source through a mask by rotating the rod through a specific angle to expose each area.[13] Micro-dimple arrays with a feature diameter of 40 μm were prepared on the outer surface of the cylinder. Zhu et al. developed a low-cost modified TMEMM method for the preparation of micro-dimple arrays on non-planar surfaces.[14] However, their approach cannot be used to fabricate micro-dimple arrays on the scale of tens of micrometers, because the minimum hole size of the mask is 100 μm. Landolt et al. reported that with the use of oxide film laser lithography instead of a conventional photoresist technique, it might be possible to fabricate micro-dimple arrays on a non-planar surface by electrochemical micromachining.[15]

Micro-dimple arrays need to be produced not only on the outer surface of a hollow cylinder, but also on its inner surface. However, all of the reports mentioned above were concerned with the fabrication of micro-dimple arrays on outer surfaces, and, to our knowledge, little has been published about the fabrication of micro-dimple arrays on inner surfaces. In this paper, we focus on the preparation of micro-dimple arrays on cylindrical inner surfaces by TMEMM.

Dry-film photoresists (acrylate-based photopolymers) have been used as masks for powder blasting, to define microfluidic channels, and as electroplating molds for the LIGA process.[16,17] These films have excellent flexibility, and the study reported here exploits this property by using a patterned dry-film photoresist to cover the inner surface of a cylinder and act as a mask during fabrication of a micro-dimple array on the surface by electrochemical micromachining.

2. Fabrication of a dry film with micro-sized through-holes

The following procedure (illustrated in Fig. 1) was used to prepare the dry film with micro-sized through-holes: ① O_2 plasma treatment for 3 min was first used to clean the substrate; ② the dry film was then laminated onto the substrate; ③ a UV oven was employed to expose the dry film through a photomask; ④ the dry film was then developed for 1 min in an aqueous solution of sodium potassium carbonate at a concentration of 1% by weight at 30 °C; ⑤ finally, the patterned dry film was peeled from the substrate and then applied to the workpiece surface. It is worth noting that no baking step is required in this procedure, which results in a reduction in processing time.

It has been demonstrated that the diameter of the holes formed in a photoresist is determined by the light energy reaching the latter, and hence by the exposure dose. An inappropriate choice of exposure dose and exposure time can result in the occurrence of blind holes in the dry film, as shown in Fig. 2.

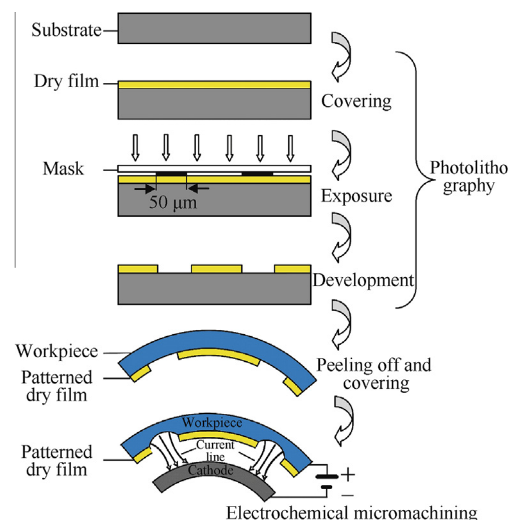

Fig. 1 Through-mask electrochemical micromachining process with a patterned dry film.

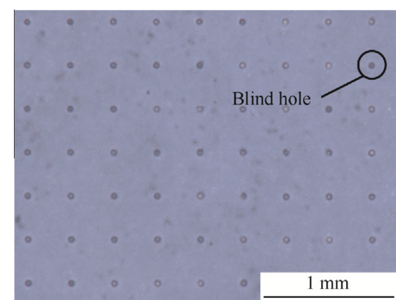

Fig. 2 An example of a blind hole in dry film.

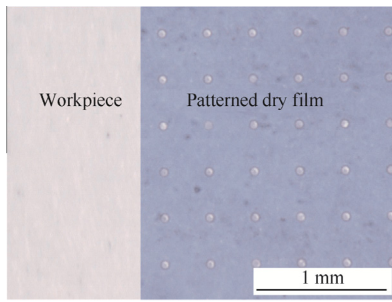

Fig. 3 Patterned dry film covering workpiece surface.

In this study, a GPM200 dry film (DuPont, USA) was employed, with an exposure dose of 70 mJ/cm^2. The GPM200 dry film is a negative photoresist, and the chemical reaction that occurs during exposure makes the photoresist insoluble in the alkaline sodium potassium carbonate solution that is used to remove the unexposed areas of the dry film. Fig. 3 shows the patterned dry film coated onto the surface of a workpiece.

3. Analysis of the current density distribution for different inter-electrode gaps

To determine the inter-electrode gap for the experiments, the effect of different gap sizes on the distribution of the current density on the workpiece was simulated.

The electric potential ϕ in the inter-electrode gap satisfies Laplace's equation

$$\nabla^2\phi = 0 \tag{1}$$

with the following boundary conditions:[12]

$$\begin{cases} \phi|_{\Gamma_1} = U(\text{at anode surface}) \\ \phi|_{\Gamma_5} = 0(\text{at cathode surface}) \\ \left.\dfrac{\partial\phi}{\partial n}\right|_{\Gamma_{2,3,7,8}} = 0 \\ \left.\dfrac{\partial\phi}{\partial n}\right|_{\Gamma_{4,6}} \approx 0 \end{cases} \tag{2}$$

where U is the applied voltage, Γ_n is the boundary, and n = 1,2,. . .,8.

The relationship between the current density i and the electric potential is

$$i = -\kappa|\nabla\phi| \tag{3}$$

where κ is the electrical conductivity of the electrolyte.

The trench-like structure is shown in Fig. 4, where D is the diameter of the holes in the dry film, H the thickness of the dry film, and G the inter-electrode gap. The model was analyzed using a finite element method, with dimensions D = 50 μm, H = 50 μm, and different values of the inter-electrode gap G = 100, 500, 1000, 5000 μm. The variation of the current density with X for different values of G (at the same applied voltage) is shown in Fig. 5, from which it can be seen that the distribution of the current density on the surface is uneven, with the lowest density occurring at the center of the trench. To ascertain the effect of G on the current density distribution, a normalized current density was defined as i/i_{max}, where i is the current density at a point on the surface and i_{max} is the maximum current density,[18] and it can be seen from Fig. 6 that this normalized current density is essentially the same for all values of G. Thus, the inter-electrode gap has a negligible influence on the current density distribution on the surface of the workpiece and can therefore be chosen arbitrarily. For this study, a value of 1 mm was used.

4. Experimental

Fig. 7 shows a schematic diagram of the experimental setup for the generation of micro-dimple arrays on the cylindrical inner

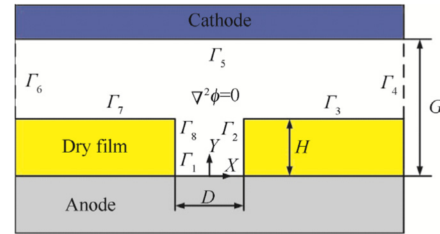

Fig. 4 Model of electric potential distribution.

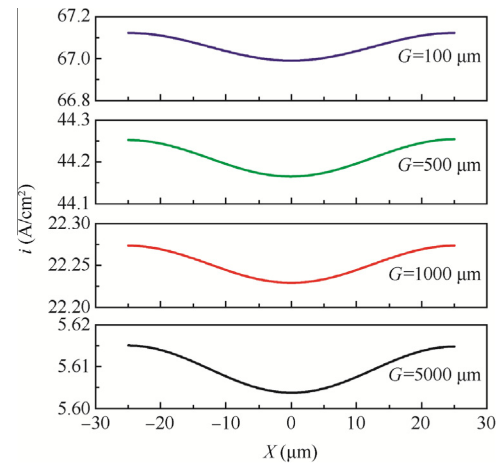

Fig. 5 Current density distribution for different values of inter-electrode spacing G.

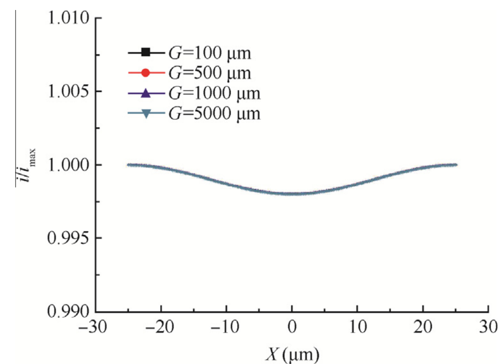

Fig. 6 Normalized current density distribution on workpiece surface.

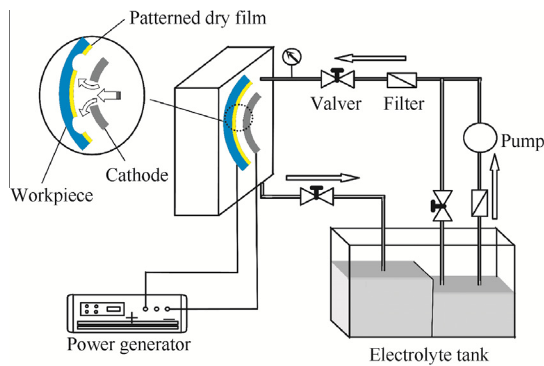

Fig. 7 Schematic diagram of experimental setup.

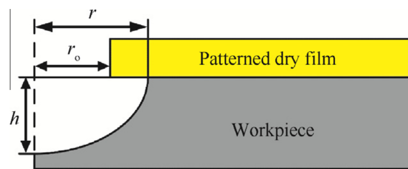

Fig. 8 Schematic diagram showing dimensions involved in definition of machining localization.

surface of a workpiece. The operations were carried out with 20 g/L sodium nitrate electrolyte, which was pumped at a pressure of 0.1 MPa. The resulting through-holes of the patterned dry film were 50 μm in diameter. The profiles of the micro-
dimple arrays were determined using a three-dimensional profilometer (DVM5000, Leica, Germany). A scanning electron microscope (S-3400 N, Hitachi, Japan) was also used to examine the arrays.

Machining localization, EF, is an important index for the micro-dimpling process, and is defined as

$$\mathrm{EF} = \frac{h}{r - r_o} \tag{4}$$

where h and r are the depth and radius of the micro-dimple, respectively and r_o is the radius of the mask hole (see Fig. 8).

5. Results and discussion

5.1. Effect of applied voltage and machining time on the micro-dimple array

In this experiment, both applied voltage and machining time were investigated to achieve high machining localization with a small dimple diameter. Factor experiments were performed, as presented in Table 1.

Table 1 Machining parameters and levels.

Parameter	Level			
	1	2	3	4
Applied voltage (V)	8	10	12	
Machining time (s)	3	5	7	9

The ranges for the diameter, depth, and EF achieved by TMEMM with the patterned dry film were analyzed, giving the results shown in Tables 2 and 3. These data reveal that machining time is the significant factor with respect to influencing machining depth and EF, while the current density has the greatest influence on machining diameter. Fig. 9 shows the influence of applied voltage and machining time on dimple dimensions. It can be seen that with increasing applied voltage, both the diameter and the depth of the dimple rapidly enlarge, while EF decreases. Moreover, it can be seen that dimple diameter, dimple depth, and EF all increase with increasing machining time, with the diameter and depth varying more slowly. It is well- known that the electric intensity on the workpiece is inversely proportional to the inter-electrode gap.[19] With the electrode arrangement of the modified TMEMM method, the inter-electrode gap increases with prolonged machining time, which will act to slow the machining rate. Considering the data from Table 3 and Fig. 9, it can be seen that to obtain micro-dimples with small diameters, a combination of a lower current density with a longer machining time is advantageous. In other words, machining localization is enhanced by reducing the applied voltage and prolonging the machining time.

It has previously been found that both applied voltage and machining time have a significant influence on dimple dimensions.[20–22] However, up to now, no definitive conclusions have been drawn regarding which combination—lower current density with prolonged machining time or higher current density with reduced machining time—is the better approach to enhance machining localization. The results reported here are the first to indicate that a lower current density with a prolonged machining time can improve machining localization. Fig. 10 shows the profiles of micro-dimples with similar depth generated at different voltages. It can be seen that for the same depth, the use of a lower voltage produces a smaller-diameter dimple.

To further investigate the apparent enhancement of machining localization by reduced applied voltage and prolonged machining time, the effect of applied voltage on the current density distribution on a micro-dimple surface with a dimple diameter of 100 μm, produced using a patterned dry-film photoresist with through-holes 50 μm in diameter, was examined. Fig. 11 shows a schematic diagram of the machined micro-dimple and Fig. 12(a) shows numerical simulations of the current density distribution on the micro-dimple surface for different applied voltages. It can be seen that the current density increases with applied voltage. According to Faraday's law, the rate of removal of material is proportional to the current density,[23] and the use of a 12 V applied voltage reduces the machining time for preparing a micro-dimple compared with an 8 V applied voltage. Fig. 12(b) shows the normalized current density distribution on the micro-dimple profile. It indicates that the profile prepared with 8 V is almost the same as that prepared with 12 V. However, the current density at point A is obviously lower than that at point C (see Fig. 11 and Fig. 12(a)), and the current density at point A obtained with 8 V is also significantly lower than that obtained with 12 V (Fig. 12(a)). A current valve is employed in our experiment because a passivating sodium nitrate electrolyte is used. When the current density at point A is close or equal to the value of the current valve, the dissolution of material at point A will weaken or stop. Meanwhile, the dissolution of material at point C will continue. Thus, machining localization is

Table 2 Response of factors under investigation to dimple dimensions.

Experiment no.	Applied voltage (V)	Machining time (s)	Dimple diameter (μm)	Dimple depth (μm)	Machining localization, EF
1	1	1	75	6.4	0.512
2	1	2	84	11.4	0.670588235
3	1	3	91	16	0.780487805
4	1	4	98	18.5	0.770833333
5	2	1	85	7.5	0.428571429
6	2	2	90	13.3	0.665
7	2	3	95	17.3	0.768888889
8	2	4	102	19.8	0.761538462
9	3	1	94.4	9.8	0.441441441
10	3	2	110	16.75	0.558333333
11	3	3	117.5	21	0.622222222
12	3	4	123	24	0.657534247

Table 3 Analysis of ranges for dimple dimensions.

Factor	Applied voltage (V)	Machining time (s)
Diameter	96.9	68.6
Depth	19.25	38.6
EF	0.45	0.81

enhanced by reducing the applied voltage and prolonging the machining time.

5.2. Fabrication of micro-dimple arrays on cylindrical inner surfaces

A patterned dry-film photoresist with through-holes 50 μm in diameter was fabricated and coated onto a cylindrical inner surface, as shown in Fig. 13. Micro-dimple arrays were then fabricated using the TMEMM process. Fig. 14(a) shows such an array produced at an applied voltage of 8 V and a machining time of 9 s. Fig. 14(b) shows an SEM image of the array and Fig. 14(c) the surface profile of a micro-dimple, which is 94 μm in diameter and 22.7 μm in depth.

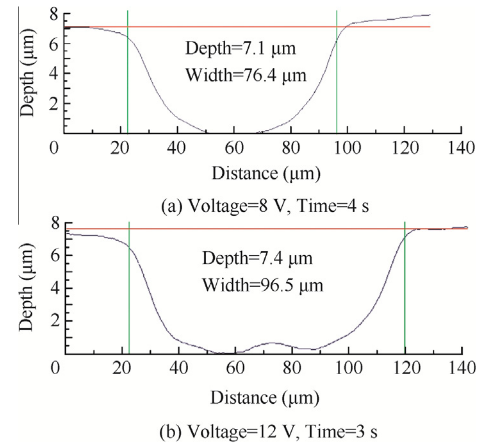

Fig. 10 Profiles of micro-dimples with similar depth generated at different voltages.

As already mentioned in the introduction, Wang and co-workers [13] have described a method for fabricating micro-dimple arrays on cylindrical outer surfaces using proximity

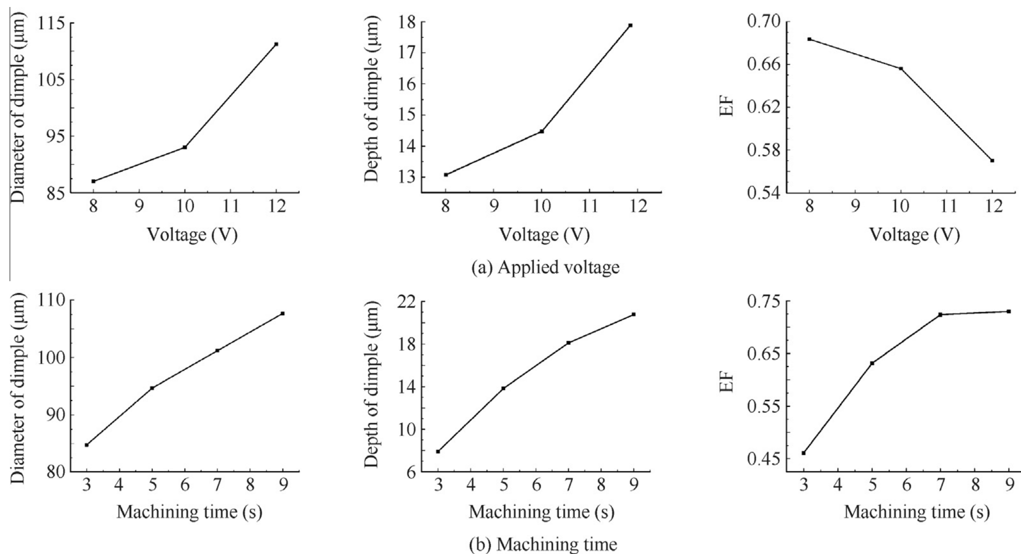

Fig. 9 Effect of applied voltage and machining time on micro-dimple dimensions.

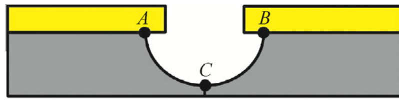

Fig. 11 Schematic diagram of a machined micro-dimple.

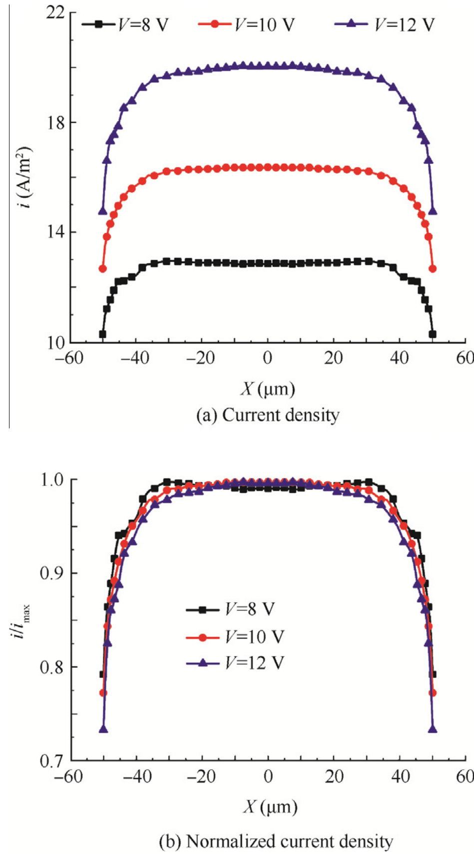

(a) Current density

(b) Normalized current density

Fig. 12 Distribution of current density and normalized current density on micro-dimple profile generated with different applied voltages.

Fig. 13 Patterned dry-film photoresist with through-holes 50 μm in diameter coated onto a cylindrical inner surface.

rolling-exposure lithography and electrochemical micromachining. However, it is not fit to fabricate micro-dimple arrays on cylindrical inner surfaces, because photoresist coating and lithography could not be achieved on cylindrical inner surfaces. The method that we have presented here can also be used on cylindrical inner surfaces. Compared with their presented method, ours is not only simpler but also cheaper. It is also worth noting that the machining time to prepare hundreds of micro-dimples by the present method is only 9

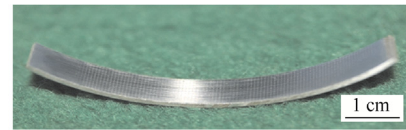

(a) Micro-dimple array on a cylindrical inner surface

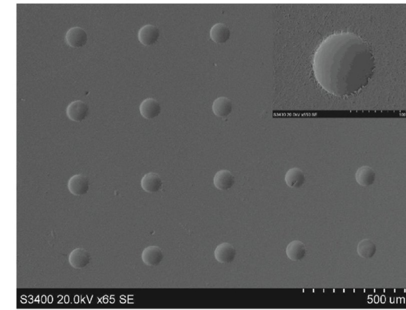

(b) SEM image of the array

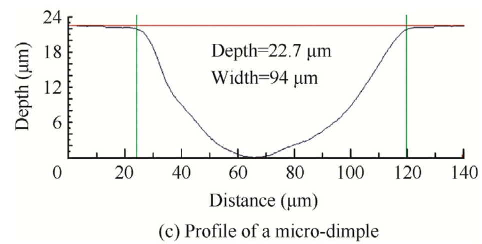

(c) Profile of a micro-dimple

Fig. 14 Machined micro-dimple array by TMEMM with dry film.

s, suggesting that it could be used to fabricate micro-dimple arrays with low cost and high efficiency.

6. Conclusions

In the experiments described in this paper, a dry-film photoresist was used as a mask for the production of micro-dimple array on cylindrical inner surfaces by TMEMM. The following conclusions can be drawn from the results of these investigations:

(1) The method presented here is capable of fabricating micro-dimple arrays on cylindrical inner surfaces with low cost and high efficiency.
(2) At a fixed dimple depth, the use of a lower applied voltage with a prolonged machining time is advantageous for obtaining small diameters.
(3) Micro-dimple arrays measuring 94 μm in diameter and 22.7 μm in depth were successfully prepared on cylindrical inner surfaces at an applied voltage of 8 V and a machining time of 9 s.

Acknowledgments

The work was supported by the Joint Funds of the National Natural Science Foundation of China and Guangdong Province (No. U1134003).

References

1. Kligerman Y, Etsion I, Shinkarenko A. Improving tribological performance of piston rings by partial surface texturing. *J Tribol-T ASME* 2005;**127**(3):632–8.
2. Nakano M, Korenaga A, Korenaga A, Miyake K, Murakami T, Ando Y, et al. Applying micro-texture to cast iron surfaces to reduce the friction coefficient under lubricated conditions. *Tribol Lett* 2007;**28**(2):131–7.
3. Bruzzone AAG, Costa HL, Lonardo PM, Lucca DA. Advances in engineered surfaces for functional performance. *CIRP Ann – Manuf Technol* 2008;**57**(1):750–69.
4. Greco A, Raphaelson S, Ehmann K, Wang QJ, Lin C. Surface texturing of tribological interfaces using the vibromechanical texturing method. *J Manuf Sci E-T ASME* 2009;**131**(6):061005–8.
5. Bao HQ, Xu JW, Li Y. Aviation-oriented micromachining technology—micro-ECM in pure water. *Chin J Aeronaut* 2008;**21**(5):455–61.
6. Rajurkar KP, Zhu D, Mcgeough JA, Kozak J, Silva AD. New developments in electro-chemical machining. *CIRP Ann – Manuf Technol* 1999;**48**(2):567–79.
7. Zhu D, Zhu D, Xu ZY, Zhou LS. Trajectory control strategy of cathode in blisk electrochemical machining. *Chin J Aeronaut* 2013;**26**(4):1064–70.
8. Natsu M, Ikeda T, Kunieda M. Generating complicated surface with electrolyte jet machining. *Precis Eng* 2007;**31**(1):33–9.
9. Nouraeiz S, Roy S. Electrochemical process for micropattern transfer without photolithography: a modeling analysis. *J Electrochem Soc* 2008;**155**(2):D97–103.
10. Costa HL, Hutchings IM. Development of a maskless electrochemical texturing method. *J Mater Process Technol* 2009;**209**(8):3869–78.
11. Byun JW, Shin HS, Kwon MH, Kim BH, Chu CN. Surface texturing by micro ECM for friction reduction. *Int J Precis Eng Manuf* 2010;**11**(5):747–53.
12. Qian SQ, Zhu D, Qu NS, Li HS, Yan DS. Generating microdimples array on the hard chrome-coated surface by modified through mask electrochemical micromachining. *Int J Adv Manuf Technol* 2010;**47**(Supply1):1121–7.
13. Hao XQ, Wang L, Wang QD, Guo FL, Tang YP, Ding YC, et al. Surface micro-texturing of metallic cylindrical surface with proximity rolling-exposure lithography and electrochemical micromachining. *Appl Surf Sci* 2011;**257**(21):8906–11.
14. Zhu D, Qu NS, Li HS, Zeng YB, Li DL, Qian SQ. Electrochemical micromachining of microstructures of micro hole and dimple array. *CIRP Ann – Manuf Technol* 2009;**58**(1):177–80.
15. Landol D, Chauvy PF, Zinger O. Electrochemical micromachining, polishing and surface structuring of metals: fundamental aspects and new developments. *Electrochim Acta* 2003;**48**(20–22):3185–201.
16. Kukharenka E, Farooqui MM, Grigore L, Kraft M, Hollinshead N. Electroplating moulds using dry film thick negative photoresist. *J Micromech Microeng* 2003;**13**(4):S67–74.
17. Vulto P, Glade N, Altomare L, Bablet J, Tin LD, Medoro G, et al. Microfluidic channel fabrication in dry film resist for production and prototyping of hybrid chips. *Lab Chip* 2005;**5**(2):158–62.
18. Zhu D, Zeng YB. Micro electroforming of high-aspect-ratio metallic microstructures by using a movable mask. *CIRP Ann – Manuf Technol* 2008;**57**(1):227–30.
19. Hackert-Oschaetzchen M, Martin A, Meichsner G, Zinecker M, Schubert A. Microstructuring of carbide metals applying Jet Electrochemical Machining. *Precis Eng* 2013;**37**(3):621–34.
20. Shin HS, Chung DK, Park MS, Chu CN. Analysis of machining characteristics in electrochemical etching using laser masking. *Appl Surf Sci* 2011;**258**(5):1689–98.
21. Wang QD, Xiao JM, Lu YJ. Numerical and experimental study on fabrication of microstructure array with topographical gradient via through-mask EMM. *Adv Mater Res* 2012;**528**:254–8.
22. Kikuchi T, Wachi Y, Sakairi M, Suzuki RO. Aluminum bulk micromachining through an anodic oxide mask by electrochemical etching in an acetic acid/perchloric acid solution. *Microelectron Eng* 2013;**111**:14–20.
23. Qu NS, Fang XL, Li W, Zeng YB, Zhu D. Wire electrochemical machining with axial electrolyte flushing for titanium alloy. *Chin J Aeronaut* 2013;**26**(1):22–49.

Qu Ningsong is a professor and Ph.D. supervisor at College of Mechanical and Electrical Engineering, Nanjing University of Aeronautics and Astronautics, China. He received the Ph.D. degree from the same university. His current research interests are electrochemical machining, electroforming, and micro electrochemical machining.